16th European Signal Processing Conference (EUSIPCO 2008), Lausanne, Switzerland, August 25-29, 2008, copyright by EURASIP

INPAINTING USING GEOMETRICAL GROUPLETS

Aldo Maalouf, Philippe Carré, Bertrand Augereau, Christine Fernandez-Maloigne

XLIM laboratory, UMR CNRS 6172, Signal-Image-Communication Department
University of Poitiers,
SP2MI-2 Bd Marie et Pierre Curie, PO Box 30179
86962 Futuroscope Chasseneuil, France
{maalouf, carre, augereau, fernandez}@sic.sp2mi.univ-poitiers.fr

ABSTRACT

In this paper, we propose a two-steps image inpainting algorithm that relies on geometrical grouplets. The grouplet orthogonal bases, that were introduced by Mallat in [1], are constructed with multiscale association field that groups pixels to take advantage of geometrical image regularities. These bases are used to represent the complex geometry of the image to be inpainted. Having well represented the image geometry by using geometrical grouplets, missing data are synthesized by propagating the geometrical information from outside to the inside of the inpainting zone. The first step of the algorithm consists of computing the multiscale association field and the grouplet transform of the image. In the second step, the integral curves of the association field are computed and propagated inside the inpainting zone to fill in the missing data. This step is accomplished by minimizing a functional whose role is to reconstruct the missing or damaged zone independently of the size and topology of the inpainting domain. Extensive experiments are carried out in order to validate and compare the algorithm both quantitatively and qualitatively. They show the advantages of our algorithm and its readily application to real world cases.

1. INTRODUCTION

Image inpainting is the process of filling in damaged or missing regions of an image with the use of information from surrounding areas. Its typical applications include restoration of old paintings and removing scratches from photographs.
The first work on inpainting was introduced by Bertalmio et al. in [2]. Their model is based on nonlinear partial differential equations, and imitates the techniques of artists specialized in restoration. Their algorithm is based on the propagation of sharp edges into the damaged parts that need to be filled in.
Subsequently, Bertozzi et al. [3] realized that there exists a connection between the work presented in [2] and the 2D fluid dynamics through the Navier-Stokes equation. Indeed, the steady-state equation proposed in [2] is equivalent to the Euler equations from incompressible flow, in which the image intensity function plays the role of the stream function in the fluid problem.
Then, a different approach to inpainting was proposed by Chan and Shen [4]. They introduced the idea that well-known variational image denoising and segmentation models can be adapted to the inpainting task by a simple modification. Their first algorithm was based on the total variation denoising approach presented in [5]. This model can successfully propagate sharp edges into the inpainting zone. However, because of the regularization term, the model imposes a penalty on the length of edges, and thus, the inpainting model cannot connect contours across very large distances.
Subsequently, Chan et al. [6] introduced a new variational image inpainting model that coped the problems of the total variation based approach. Their method includes a regularization term that penalizes not merely the length of edges in an image, but the integral of the square of curvature along the edge contours. This allows both for isophotes to be connected across large distances, and their directions to be kept continuous across the edge of the inpainting region. The major drawback of this approach is that it suffers from oversmoothing effect, especially when the regions to be filled are thick.
Subsequently, Elad. et al. proposed in [12] an inpainting technique based on a decomposition in a curvelet basis. In this method, the image is decomposed into two components: the texture content and the cartoon content using the curvelet transform. Then, the total variation approach proposed in [5] is used to fill in the missing regions. This step is performed on both image components. This approach allows for recovering missing textures data and fine edges, however, its major drawback is that it does not allow to connect contours across large distance due to the regularization term.
Recently, Bertalmio [8] proposed a new partial differential equation (PDE)-based method for inpainting that is based on the idea that the inpainting problem is non other a particular case of image interpolation in which we intend to propagate level lines. By expressing this in terms of local neighborhoods and by using a Taylor expansion, he derived a third-order PDE that performs inpainting. The third-order PDE ensures continuation of level lines, which in turn, allows the restoration of thin structures occluded by a wide gap.
In [9], Wang et al. proposed an inpainting technique that is based on the propagation of isophotes. Their method is simple and preserves sharp edges. However, it is unable to remove artifacts like the discontinuous patterns.
Afterward, Bertozzi et al. proposed in [10] an inpainting technique based on the Cahn-Hilliard equation. Their method showed good results in inpainting of degraded text, as well as superresolution of high contrast images. Still, it showed some limitations in inpainting large areas.
In this paper, we propose an inpainting approach that is based on geometrical grouplets. It consists of two steps. First, the integral curves of geometric association field of different zones of the image are determined and the grouplet transform is computed. This step allows a better representation of the multiscale geometry of the image's structures than other representation such as the wavelet transform and the bandelet transform (refer to [1] for a comparison between different geometrical representations). Having well represented this ge-

ometry, the information inside the inpainting domain is synthesized by propagating the geometric flow curves inside that zone.
Geometrical grouplets offer more flexibility in the sense that we can define geometry along flow lines that are not parallel. This geometrical representation converges toward singularities. Therefore, fine structures are well represented, and the propagation of the represented geometrical data in the inpainting region guarantees an efficient reconstruction of the missing data as the experimental results showed.
The rest of the paper is organized as follows. In section 2 a review of the grouplet transform is given. In section 3 the inpainting technique is described. Section 4 is devoted for experimental results and section 5 is a conclusion.

2. GEOMETRICAL GROUPLETS

Geometrical grouplets have been recently introduced by Mallat in [1]. They are constructed with association fields that group points to take advantage of geometrical image regularities. We only present here a brief review of the Grouplet transform. The reader can refer to [1] for a full detailed description of the Grouplet transform.
Grouplet transform uses a multiscale association field in order to group together wavelet coefficients in the direction specified by the flow [1]. These recursive groupings allow to take into account junctions and long range regularities of images.
The geometrical grouplet transform is first computed by performing group matching on the 2D wavelet transform of the image in order to obtain the association field. The role of this field is to group together points that have similar neighborhoods in order to exploit the geometry of the image. The computation of the association field is performed as follows: First the image grid Ω is divided into two subgrids Ω_{even} (even columns) and Ω_{odd} (odd columns) then, each point in the odd subgrid is associated to a point in the even subgrid according to a block matching criteria (refer to [1]for more details). Then, a weighted Haar lifting is applied successively to points that are grouped by the association field. This iterative process decomposes the original image in an orthogonal basis called grouping basis. An example of an association field computed on the Barbara image is shown in figure 1.
Compared to other geometrical representation, such as bandelet or curvelet transforms, the grouplet transform is more flexible since the association fields can deviate from the integral lines in order to converge to singularity points such as junction or crossings. Fine image structures are consequently well represented. Therefore, the propagation of the represented information in the inpainting regions of the image following the integral lines of the association field yields to a precise reconstruction of the missing data. We represent in the following section this inpainting technique.

3. INPAINTING USING GEOMETRIC GROUPLET

Given that the image geometry is very well presented and characterized by a multiscale association field, we represent in this section a geometric reconstruction method based on the propagation of the geometric data from outside to inside the inpainting region to fill-in the missing data. First, we represent some preliminaries definitions and then we describe our inpainting technique.

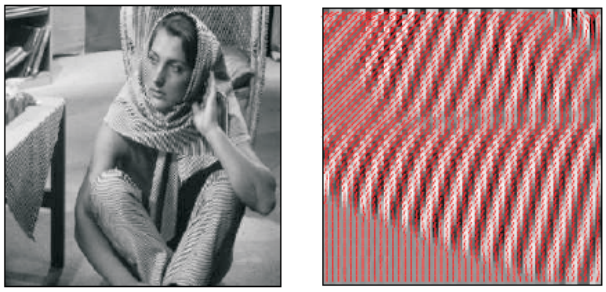

(a) (b)

Figure 1: (a) Original image, (b) a zoom on the association field of the barbara image

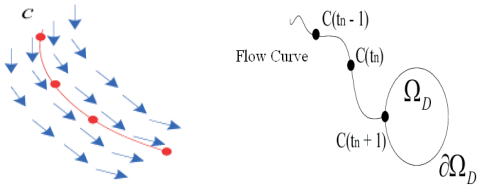

(a) (b)

Figure 2: (a) Integral lines of the association field, (b) Continuation of the integral lines of the flow

3.1 Preliminaries

The association field is expressed using n real-valued functions on $\mathbb{R}^n$. Let $f_i(\mathbf{x})$ for i from 1 to n denote such functions. Using these, the association vector field is specified as

$$f(\mathbf{x}) = [f_1(\mathbf{x}) \quad f_2(\mathbf{x}) \quad f_n(\mathbf{x}) \ ] \tag{1}$$

In this case, it appears that a vector field is a function f from $\mathbb{R}^n$ to $\mathbb{R}^n$. Therefore, standard function notation will be used from this point onward to denote the vector association field. Imagine a point that starts at some $\mathbf{x}_0 \in \mathbb{R}^n$ at time $t = 0$ and then moves according to the velocities expressed in the association field f. Its trajectory starting from $\mathbf{x}_0$ can be expressed as a function $C : [0,\infty) \to \mathbb{R}^n$, in which the domain is a time interval, $[0,\infty)$. A trajectory represents an integral curve (or solution trajectory) of the differential equations with initial condition $C(0) = \mathbf{x}_0$ if

$$\frac{dC}{dt}(t) = f(C(t)) \tag{2}$$

for every time $t \in [0,\infty)$. This could be expressed in integral form as

$$C(t) = \mathbf{x}_0 + \int_0^t f(C(s))\,ds \tag{3}$$

and is called a solution to the differential equations in the sense of Caratheodory . Intuitively, the integral curve starts at $\mathbf{x}_0$ and flows along the directions indicated by the velocity vectors (Figure 2(a)).
The integral curve C is propagated into the inpainting domain at a constant velocity.

Let the image I be a real value function on a spatial domain Ω. We designate by Ω_D the inpainting domain ($\Omega_D \subset \Omega$).

The domain Ω_D regroups the pixels of the inpainting region and $\partial\Omega_D$ denotes the border of the inpainting zone (Figure 2(b)).
The proposed model aims at recovering missing or damaged areas of an image in such a way as to tie in the integral curves of the association field along those areas.
To find the continuation of the integral curves, from outside to inside of the inpainting domain, following the direction of the association field, we propose a variational approach that is described in the next section.

3.2 The Inpainting Algorithm

In order to perform the integral curve continuation, we propose to minimize the following functional:

$$l = \int |C'(t)| dt \tag{4}$$

where $C'(t)$ is the directional derivative of C with respect to the geometrical direction θ (the direction that is induced by the association field vectors) that is determined by the grouplet transform.

$$C'(t) = (x'(t)\cos\theta, y'(t)\sin\theta)$$

To implement equation (4) to carry out the synthesis of the missing or degraded data, we propose the following algorithm:

1. Definition of the inpainting domain Ω_D.
2. Automatic detection of the points belonging to the boundary $\partial\Omega_D$. A pixel $\mathbf{x}$ belongs to the border if, and only if, it belongs to the inpainting domain and any neighborhood $V(\mathbf{x}, r)$ centered at pixel $\mathbf{x}$ and radius r ($r \geq 1$), contains at least one pixel not belonging to the inpainting domain.
3. The filling in of information on the pixels border (belonging to $\partial\Omega_D$) is performed in such a way as to satisfy the condition given by equations (4). In the numerical discretization, these conditions are reached by the following procedure.
   a. Compute the 2D orthogonal wavelet transform of the image at a scale 2^j.
   b. Compute the association field on the wavelet coefficients by first dividing each subband grid into two sub-grids called "even sub-grid" (Ω_{even}) and "odd sub-grid" (Ω_{odd}) and then associating to each wavelet coefficient m_{odd} in the odd sub-grid a coefficient m_{even} from the even sub-grid that satisfies the so called "best fit of radius P" which is defined by:

$$m_{even} = \arg\min_{m\in\Omega_{even}} \sum_{|n|<P} |a[m-n] - a[m_{odd}-n]|^2 \tag{5}$$

   c. Compute the weighted mean and difference over pairs of pixels that are neighbors according to the association field. The output of this step is a detail image and an image corresponding to low frequency components. The following steps are performed on both images.
   d. Compute the flow integral curve C at each pixel on the border $\partial\Omega_D$ from the association field.

Figure 3: Barbara image, degraded with artificial artefacts.

   e. The value transported to the pixel in question is:

$$C(t_n+1) = C(t_n) + \Delta t C'(t_n) \tag{6}$$

   where Δt is the Euclidean distance between $C(t_n+1)$ and $C(t_n)$ (see Figure 2(b)). In other word, $C(t_n+1)$ corresponds to the value of the nearest pixel, in the same direction of the flow defined by the association field and that does not belong to Ω_D, added to the value of the directional derivative with respect to the direction of the flow.
   f. Step e is repeated until the values of the boundary points do not change anymore.
   g. Compute the inverse grouplet transform.
   h. The elements modified by the transportation are excluded from the inpainting domain.
   i. If elements still exist in the new inpainting domain, go back to step 2.

4. EXPERIMENTAL RESULTS

We perform experiments to validate our algorithm and compare it with existing ones. Figure 3(a) shows an artificially degraded version of the 'barbara' image. The image is restored by using our grouplet-based inpainting technique as well as other techniques existing in the literature.

A zoom-in on three of the artefact areas in the restored images is shown in figures 4, 5 and 6. Visual inspection of these results shows that a better restoration quality is obtained by using our grouplet-based algorithm. Both sharp and smooth edges are well recovered.
Figure 7 shows additional results to remove real objects in images using the proposed algorithm. The object to be removed (the flower) is of thick shapes. The performance of different algorithms presented in the experiments can be measured by a subjective view to the results. It is clear that our algorithm outperforms other state of the art techniques in inpainting thick and normal shapes.
Besides using visual inspection, we have also assessed the performance of the algorithm in a quantitative manner. A set of experiments was performed on a set of seven 512×512 images (see the name list in the legends of Fig. 7). These images were chosen because they exhibit some local structure. We have conducted the following series of experiments for each image. Artefacts with random shapes and locations

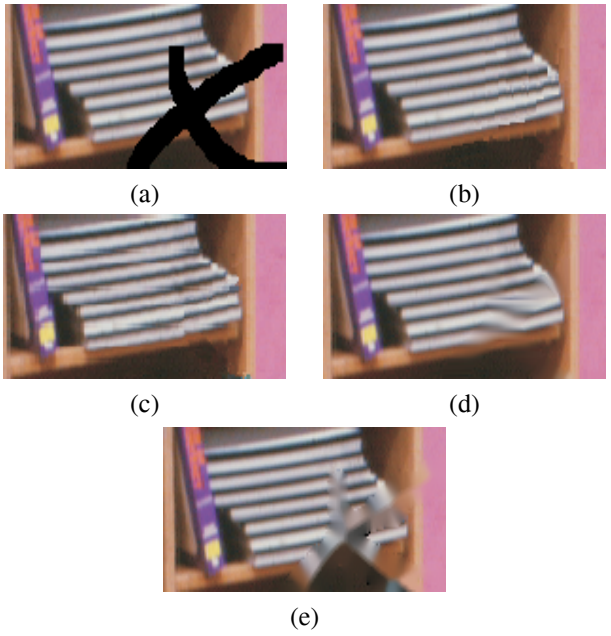

Figure 4: (a) Zoom in on the original scratched area, Zoom-in on the restored image obtained by using: (b) our groupelt-based technique, the methods of (c) Wang et al. [9], (d) Bertozzi et al. [10] and (e) Bertalmio [8]

were generated, having sizes of 1, 2, 5, 10, 20, 50, 100, 200, 500, 1000, 2000, 5000, and 10000 pixels. For each size and each image, a single artefact was generated and restored in 100 consecutive experiments (each time with a different, random shape and location). For each restoration, the mean-square error (MSE) was measured between the original and the reconstructed image. The MSE plots are shown in Fig. 7, with artefact sizes on a logarithmic scale. For each size and each image, the median MSE for the 100 experiments was plotted (this was chosen in order to avoid the influence of a small percentage of outliers). The MSE values stay within acceptable ranges, in general. A growing trend for bigger artefacts is present, as expected (the trend seems to accelerate at larger sizes because of the logarithmic scale used). From a perceptual point of view, our algorithm performed satisfactorily for MSE values up to about 0.02. Above this value, the quality of the restoration degraded in a more visible manner. This value is only a rough estimate and should not to be taken as an absolute reference, since the MSE is not strictly correlated with the visual quality. Depending on the textural content and the structural complexity of each image, the restoration errors may start becoming visible at smaller or larger MSE values and/or artefact sizes. All experiments have been done with the same parameter setting. This showed that the parameter setting was not really sensitive to different images (i.e., different structure configurations), nor to different artefact shapes.

5. CONCLUSION

In this work, a new inpainting technique is proposed, which allows to reconstruct the inpainting zone by the propagation of the geometrical information obtained by using the geometrical grouplet from outside to the inside the missing

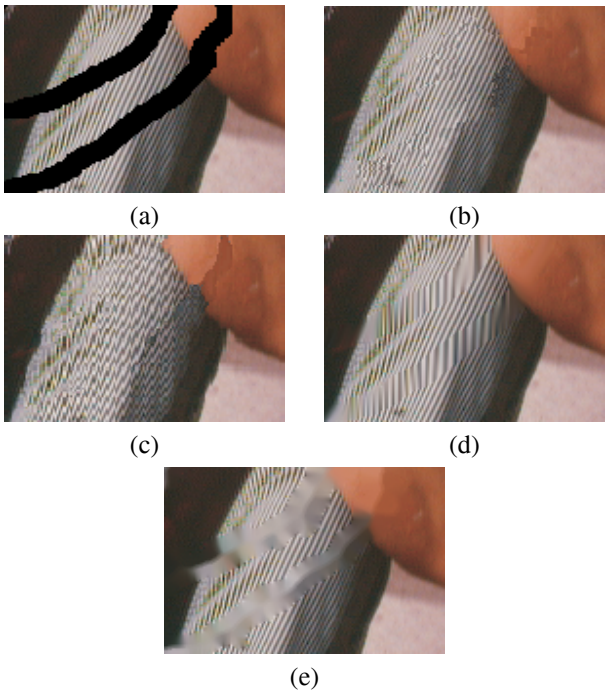

Figure 5: (a) Zoom in on the original scratched area, Zoom-in on the restored image obtained by using: (b) our groupelt-based technique, the methods of (c) Wang et al. [9], (d) Bertozzi et al. [10] and (e) Bertalmio [8]

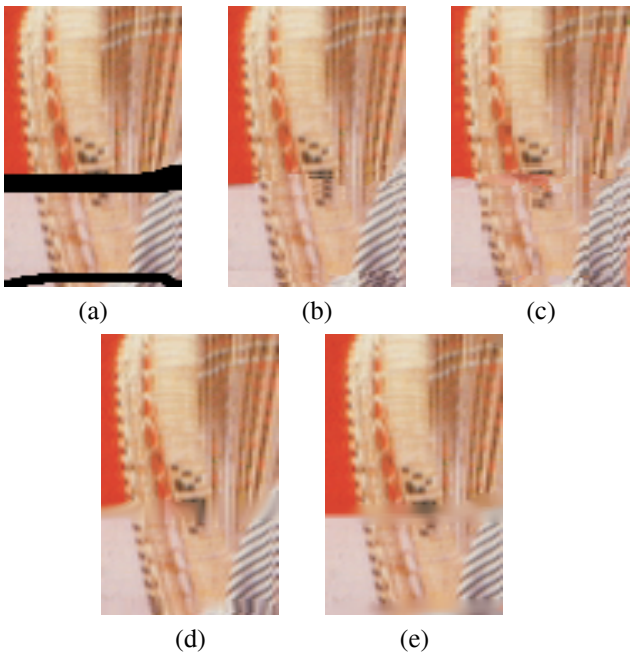

Figure 6: (a) Zoom in on the original scratched area, Zoom-in on the restored image obtained by using: (b) our groupelt-based technique, the methods of (c) Wang et al. [9], (d) Bertozzi et al. [10] and (e) Bertalmio [8]

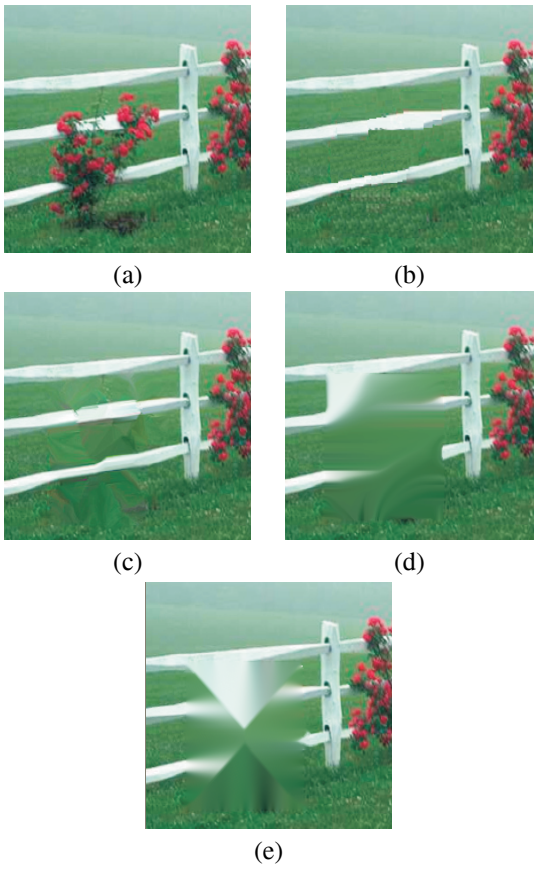

Figure 7: Inpainting to remove objects (a) original image. Restored image using: (b) Our grouplet-based technique, the methods of (c) Wang et al. [9], (d) Bertozzi et al. [10] and (e) Bertalmio [8]

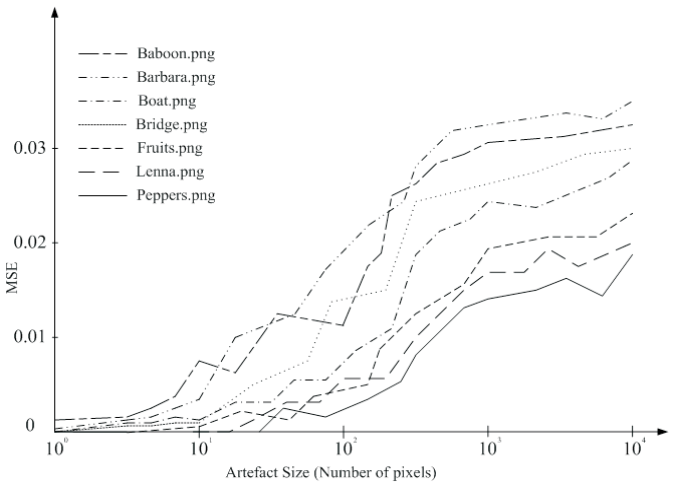

Figure 8: Plot for the experiments done on the image test set. Each point represents the median MSE of 100 experiments done on the same image, with random artefacts of the same size.

zone. The propagation of the geometrical information is performed bu the minimization of a functional. Experiment results point out the superiority of the proposed method compared to other state of the art inpainting techniques.
Finally, in order to improve the proposed inpainting method, an aspect deserves to be investigated in future research studies, which is the independent inpainting applied to each image channel. It could be improved by a joint multichannel inpainting process.

REFERENCES

[1] Stephane Mallat, "Geometrical grouplets," *Submitted to ACHA*, October 2006.

[2] G. Sapiro V. Caselles, M. Bertalmio and C. Ballester, "Image inpainting," *ACM SIGGRAPH (Addition Wesley Longman, ed.), ACM PRESS*, pp. 417–424, 2000.

[3] A. Bertozzi M. Bertalmio and G. Sapiro, "Navier stokes, fluid dynamics and image and video inpainting," *in Proc. IEEE Computer Vision and Pattern Recognition*, vol. 1, pp. 355–362, December 2001.

[4] T. F. Chan and J. Shen, "Mathematical models of local non-texture inpaintings," *SIAM J. Appl. Math.*, vol. 62, no. 3, pp. 1019–1043, 2001.

[5] S. Osher L. Rudin and E. Fatemi, "Non linear total variation based noise removal algorithms," *Phys. D*, vol. 60, pp. 259–268, 1992.

[6] S. Kang T. Chan and J. Shen, "Euler's elastica and curvature-based inpaintings," *SIAM J. Appl. Math.*, vol. 63, no. 2, pp. 564–592, 2002.

[7] H. Grossauer and O. Scherzer, "Using the complex ginzburgŰlandau equation for digital inpainting in 2d and 3d," *in Proc. Scale Space Methods in Computer Vision, Lecture notes in Computer Science*, vol. 2695, pp. 225–236, 2003.

[8] Marcelo Bertalmio, "Strong-continuation, contrast-invariant inpainting with a third-order optimal pde," *IEEE TRANSACTIONS ON IMAGE PROCESSING*, vol. 15, no. 7, pp. 1934–1938, 2006.

[9] Fugen Zhou Zhaozhong Wang and Feihu Qi, "Inpainting thick image regions using isophote propagation," *IEEE ICIP*, 2006.

[10] Selim Esedoglu Andrea L. Bertozzi and Alan Gillette, "Inpainting of binary images using the cahn-hilliard equation," *IEEE TRANSACTIONS ON IMAGE PROCESSING*, vol. 16, no. 1, pp. 285–291, 2007.

[11] G. Peyre and S. Mallat, "Discrete bandelets with geometric orthogonal filters," *Proceedings of ICIP*, September 2005.

[12] M. Elad, J-L. Starck, P. Querre and D.L. Donoho, "Simultaneous Cartoon and Texture Image Inpainting Using Morphological Component Analysis,"" *Journal on Applied and Computational Harmonic Analysis*, vol. 19, pp. 340–358, November 2005.